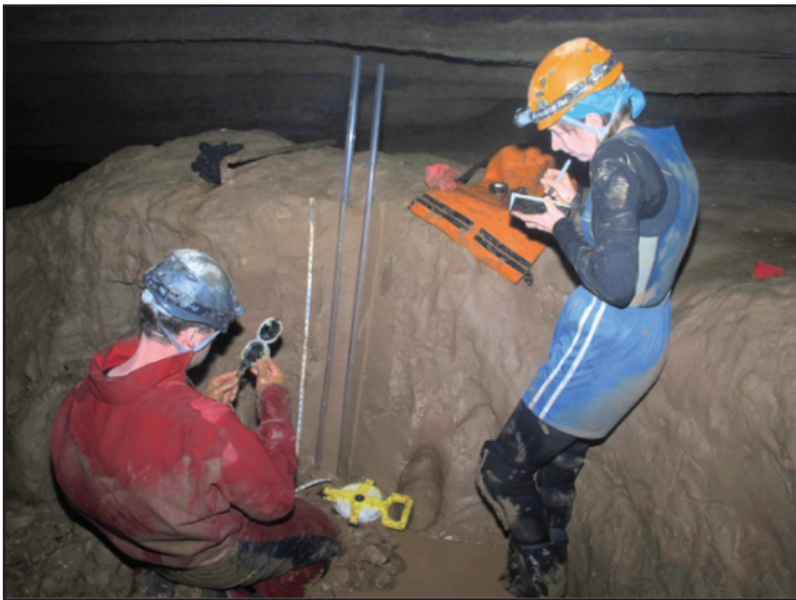


# Hydrogeology of the mantled karst of Northwest Arkansas

## 2023 Field Guide



Arkansas Field Workshop  
May 16th - 19th at the University of Arkansas  
*Carbonate Critical Zone Research Coordination Network*

## Schedule

### MAY 17TH - NWA MANTLED KARST FIELD TRIP

8:00 - 8:30	Breakfast (CORD 127)
8:30 - 9:00	Plenary session (CORD 127)
9:00 - 9:30	Drive to Savoy
9:30 - 11:15	Visit various sites at Savoy Experimental Watershed
11:15 - 12:15	Drive to Blowing Springs, Bella Vista
12:15 - 12:30	Blowing Springs field stop
12:30 - 1:00	Lunch at Blowing Springs
1:00 - 1:30	Drive to Crystal Lake
1:30-2:30	Tour Crystal Lake epikarst
2:30-3:00	Drive to Cave Springs
3:00-4:00	Visit Cave Springs
4:00-4:30	Drive back to Fayetteville
	Break
18:30 - 20:30	Dinner Banquet (Arsaga's Mill District)

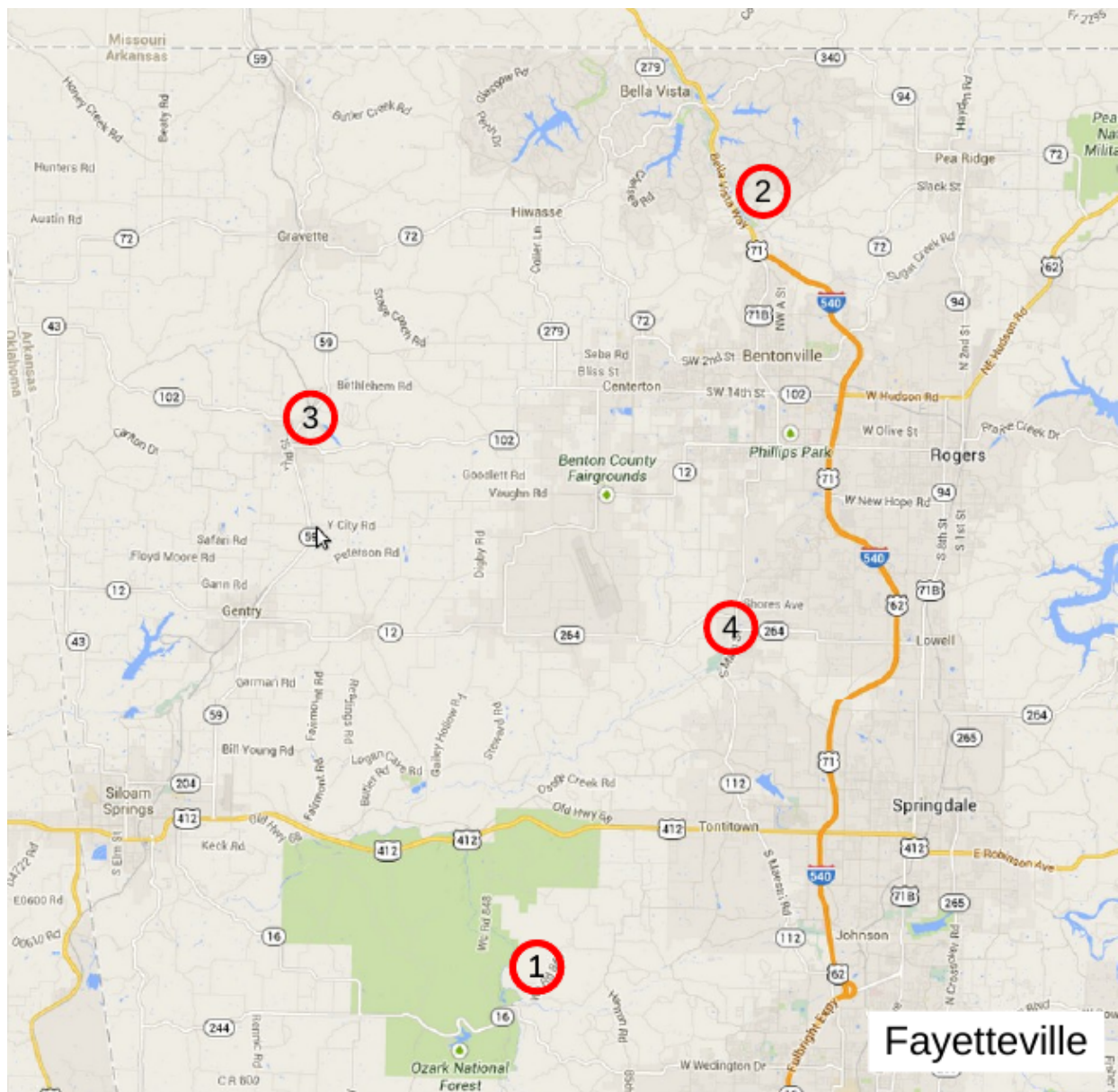


Figure 1: Locations of the field trip stops. 1) Savoy Experimental Watershed, 2) Blowing Springs, 3) Crystal Lake, 4) Cave Springs.

## Road Log

### 1. SAVOY EXPERIMENTAL WATERSHED, NEAR SAVOY, AR

The Savoy Experimental Watershed (SEW) is a collaborative Research Site for the Study of Animal Waste Management in Mantled Karst Terrains. The main goal of (SEW) is to establish and maintain a long-term research site for comprehensive, multi-disciplinary research of animal waste impacts on surface and subsurface water quality and hydrogeology. The SEW has been operational since 1996, and has a discontinuous but meaningful record of hydrologic, water quality, geologic, and soil characterization studies completed. SEW has served primarily as an applied field-training site and education and outreach center, with an impressive array of infrastructure, studies, and understanding gained from field camps, training courses, field trips, and thesis and dissertation research projects.

### 2. BLOWING SPRINGS, BELLA VISTA, AR

Blowing Springs is one of the larger springs and caves in the Bella Vista area. The spring emerges from the St. Joe Limestone. The cave is a branchwork stream cave and the passages are controlled by a mix of bedding partings and joints. The cave displays a regular pattern of chimney effect airflow with cool air blowing out of the cave entrance in the summer and cold winter air being sucked in the entrance in winter. This site has undergone extensive study over the past 15 years, with studies focusing on contaminant transport, CO<sub>2</sub> dynamics, and stable isotopes.

### 3. CRYSTAL LAKE EPIKARST

The soil and regolith cover has been removed by erosion from the overflow at Crystal Lake, exposing a subsoil karstification at the top of the St. Joe Formation (Pierson Member). The nearly orthogonal joints direct flow during times of high water, and debris in the enlarging flow passages creates a remarkably variable water level. A spring resurges from the base of the Pierson, and a well washed surface of the underlying Northview Member (shale facies) is visible. The regional confining unit, the Chattanooga Shale, is visible lower in the valley of Wolf Creek. Upstream, and behind the dam, the cherty facies of the lower Boone Formation can be seen in the far bluffs.

### 4. CAVE SPRINGS CAVE, IN CAVE SPRINGS, AR

Cave Springs Cave contains one of the largest known populations of the Ozark Blind Cavefish, which is an endangered species. This site is managed by the Arkansas Natural Heritage Commission and the Illinois River Watershed Partnership. The recharge area for the cave has undergone increasing development over the last 30 years. However, the presence of the cave fish has influenced both the location of Highway 540 and Northwest Arkansas Regional Airport.

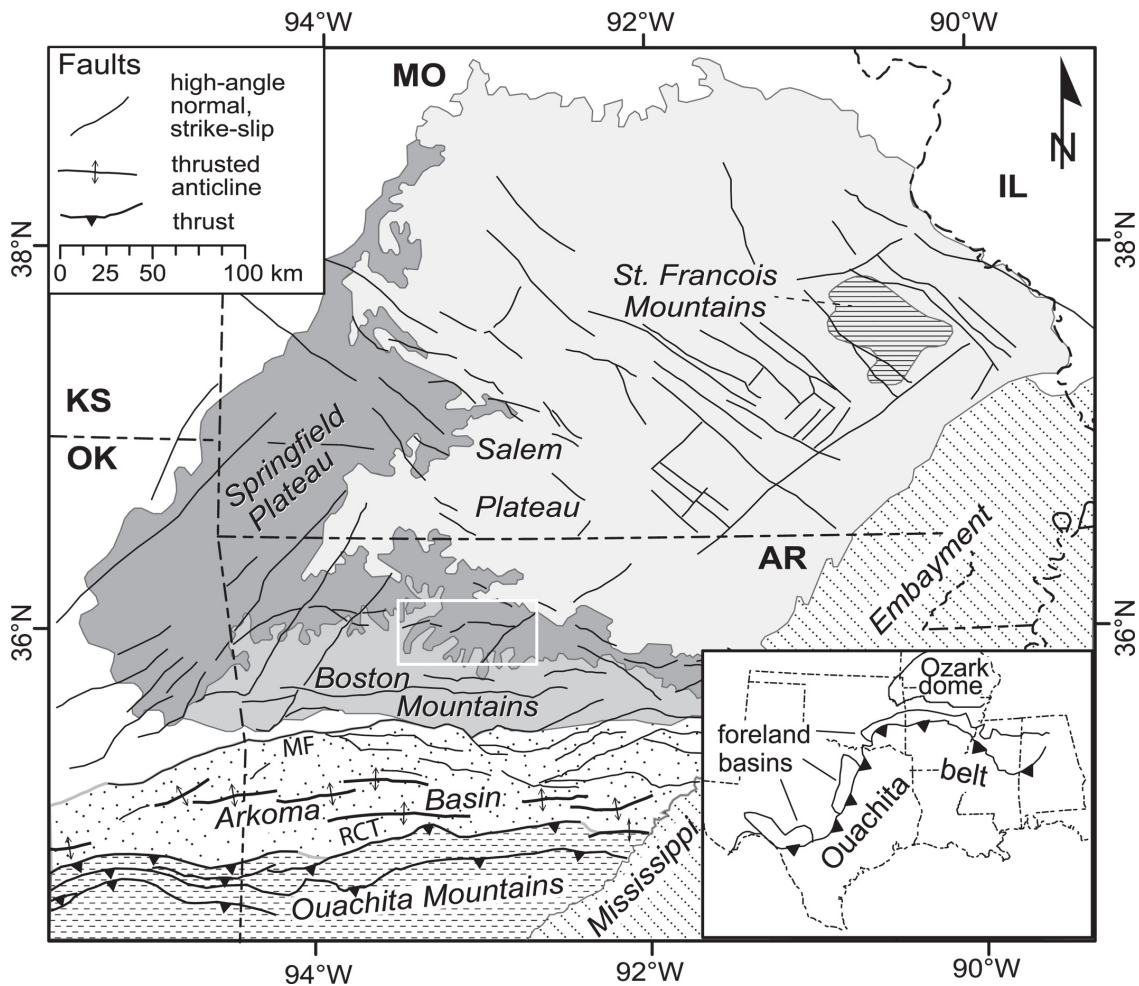


Figure 2: A map of the physiographic provinces of Northern Arkansas and Southern Missouri. From *Hudson and Turner* [2022].

## Introduction and geological context

The field trip will be located within the Ozark Plateaus region of Northern Arkansas. The Ozark Dome is in the foreland of the Late Paleozoic Quachita fold-thrust belt (Figure 2). Most of the tectonic deformation and uplift is thought to have occurred during that time [Hudson, 2000]. Modern topography is largely reflective of the sub-horizontal rock layers within the region, with the Boston Mountains being held up by erosion-resistant Pennsylvanian sandstones, the Springfield Plateau (where most of our field trip occurs) underlain by the Mississippian Boone Limestone, and the Salem Plateau being underlain by Ordovician dolomites, limestones, and sandstones. The igneous core of the Ozark Dome is exposed in the St Francois Mountains in Missouri. The southern edge of the Ozarks is bounded by the Arkoma Basin, which is the foreland basin of the Quachita Mountains. NE-SW trending faults are one of the primary results of structural deformation within NW Arkansas, and they provide important controls on karst conduit development in the region.

The rocks within the area span from Ordovician dolomites, exposed near the Missouri

border, to Pennsylvanian sandstones, which cover some of the hilltops near Fayetteville, on the edge of the Boston Mountains (Figure 3). Most of the field trip will focus on areas underlain by the Boone and St. Joe Limestones. The Boone Limestone is sometimes broken into a pure Upper Boone and a chert-rich Lower Boone. The underlying St. Joe limestone is relatively pure and is the best cave-forming unit in the region. The St. Joe is underlain by the Devonian Chattanooga Shale, which acts as an aquiclude. As a result, many springs develop near the St. Joe-Chattanooga contact.

The relatively high chert and clay content of the Boone Limestone leads to the development of a **mantled karst** landscape, where the karst surface is covered by a thick blanket of regolith, primarily composed of residual chert and clays after the limestone has dissolved away (Figure 4). This regolith can hide much of the karst nature of NWA, and surface topographic expressions of karst, such as sinkholes, are relatively rare. Here we observe a CZ setting that results from rock types that are not pure end-members on the carbonate-silicate spectrum (Figure 5).

## Savoy Experimental Watershed

The **Savoy Experimental Watershed** (SEW) is a collaborative research site for the study of nutrient management and groundwater flow in a mantled karst system [Brahana, 2011]. Since the site is also run as a cattle ranch, much of the previous work at the site has focused on the management of animal waste and nutrients in karst. The bedrock at the site spans from the Lower Boone, down into the St. Joe (where most of the springs are located) and into the Chattanooga Shale.

The groundwater basin that we will be visiting contains two base-level springs that emerge near the bottom of the St. Joe limestone, Langle Spring and Copperhead Spring. During high flow levels, both of these springs receive water from the sinking stream located near the middle of the study area (Figure 6). Copperhead and Langle Springs act as an underflow-overflow system [Brahana *et al.*, 1999; Brahana, 2011]. At low flow, all of the water from the sinking stream emerges at **Langle Spring**, which is at slightly lower elevation and is the **underflow spring**. **Copperhead Spring** is an **overflow spring**, meaning that it receives water from the sink whenever the capacity of the conduit feeding Langle Spring is overwhelmed, acting as a kind of pressure relief valve. As a result, Langle Spring has higher flow during dry conditions and somewhat limited flow variability. Copperhead Spring has very low flow during dry periods but higher flow during floods, exhibiting very high discharge variability.

The sinking stream is fed by a set of epikarst springs. It is hypothesized that these springs are perched on top of a continuous bed of chert, which stops vertical flow and directs the water down the dip and out the hillside. This water flows on the surface for only a short distance, before it sinks back into the ground and flows to Copperhead and/or Langle Spring. Some of the sink points are **estavelles**, meaning that they act as sink points during low flow and as springs during high flow. In addition to the springs and sinks, there are two wells within the study basin that will allow us to characterize groundwater further away from the main karst flow paths.

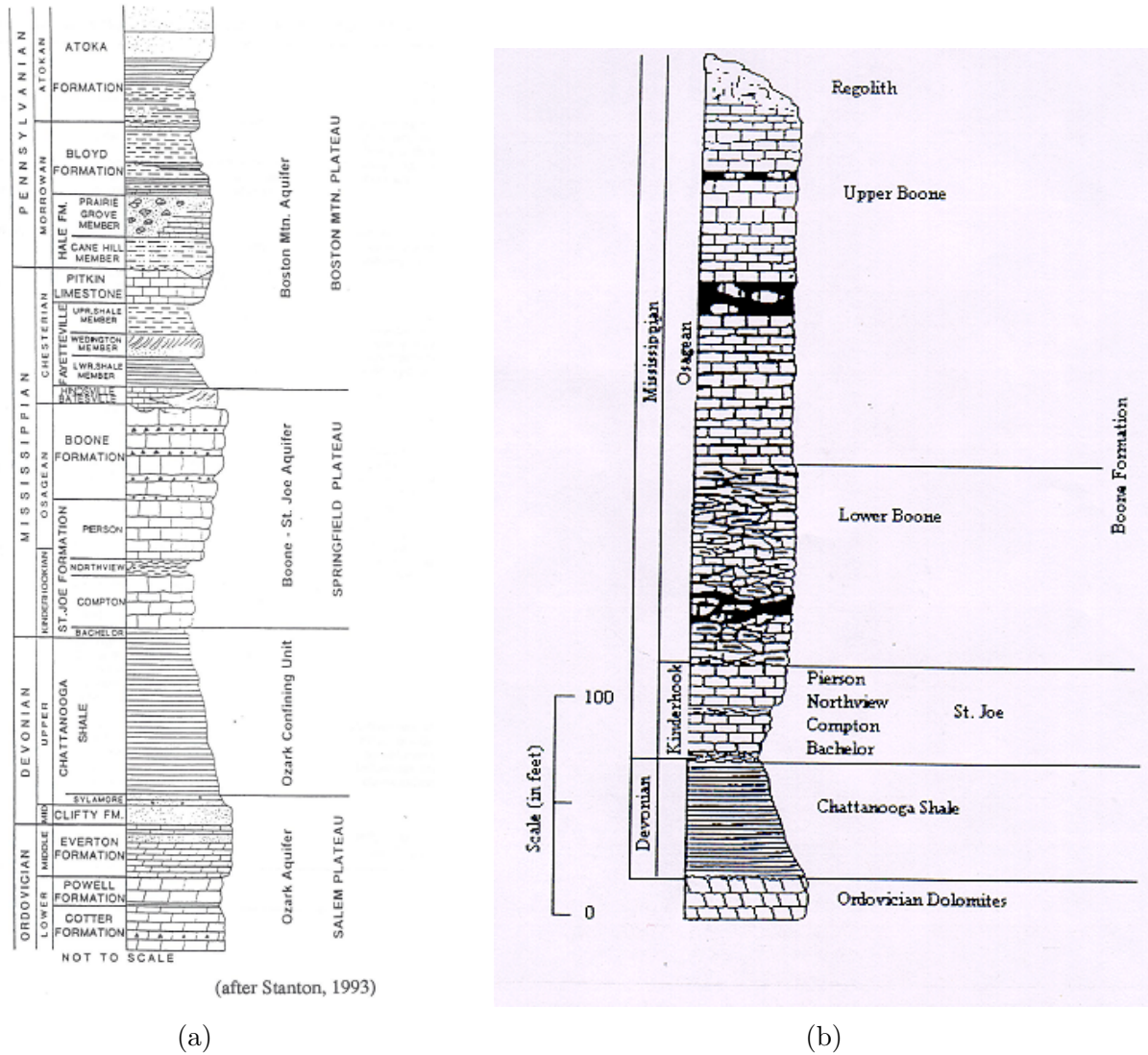


Figure 3: Stratigraphic columns of Northwest Arkansas. (a) Rocks spanning from Ordovician to Pennsylvanian outcrop in the region. (b) Zoom-in of primary rocks seen during field trip, including division of Boone into the relatively pure Upper Boone and the chert-rich Lower Boone.

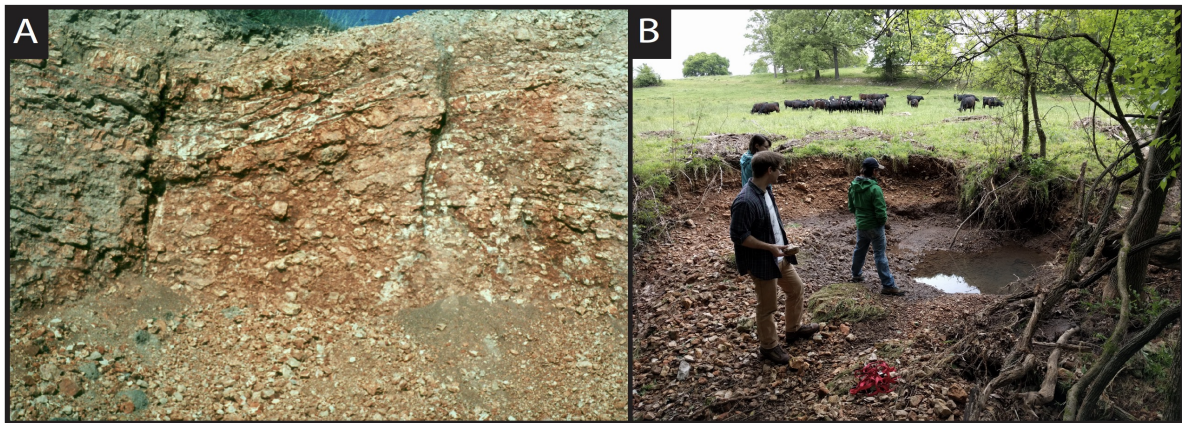


Figure 4: (A) Regolith covering the Boone Limestone in Northwest Arkansas. It is primarily composed of insoluble chert and clay minerals that are left behind when the limestone dissolves. (B) An estavelle near the sinking stream at Savoy shortly after a flood event. During low flow it is a sink point and during high flow it is a spring. Note the thick regolith cover that has been blown out during high flow.

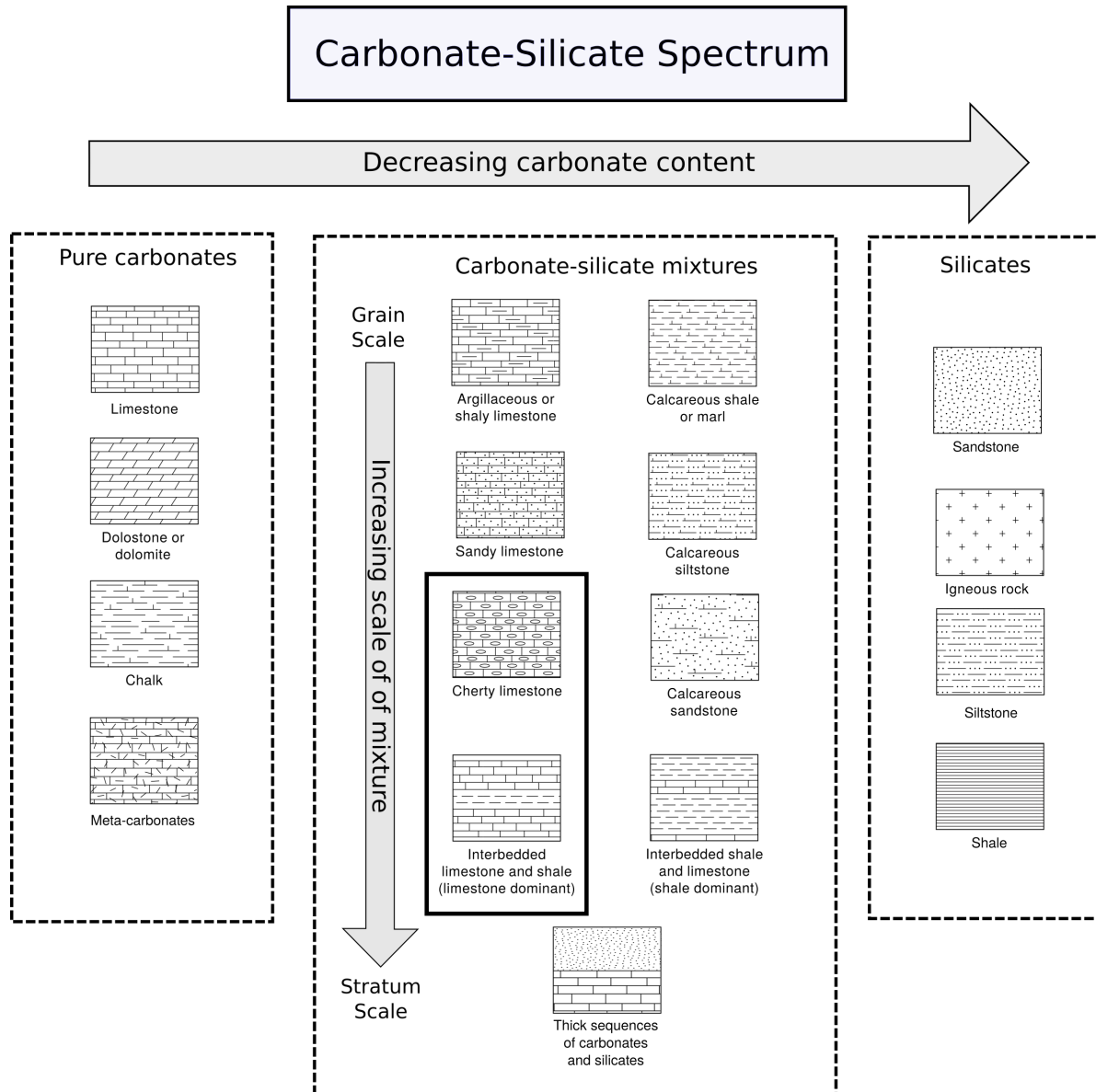


Figure 5: The carbonate-silicate spectrum. Rocks of the Ozarks are interbedded carbonates and silicates. The thickest carbonate unit, the Boone Limestone contains a substantial percentage of chert and clay. Figure modified from Covington *et al.* [2023]

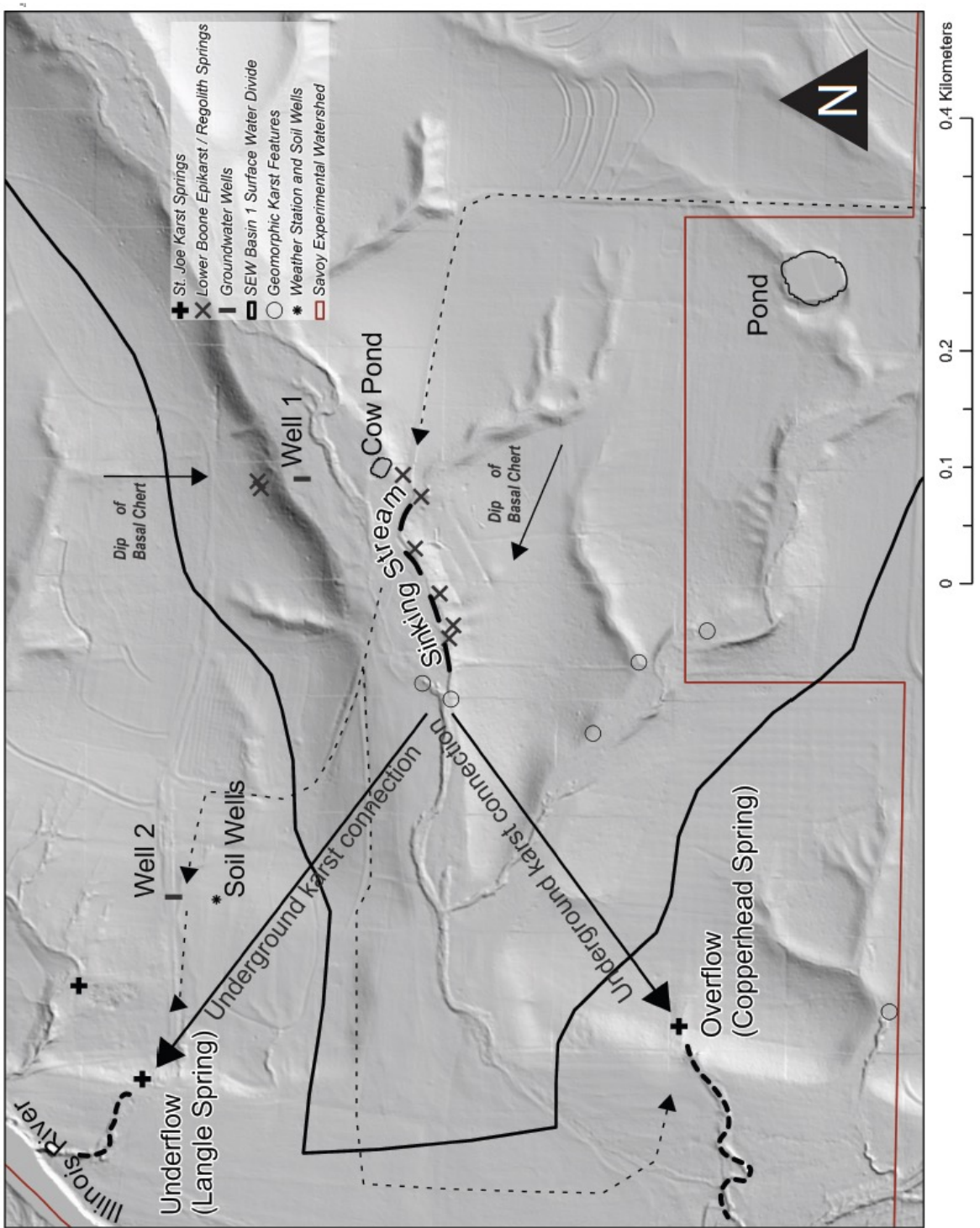


Figure 6: Study basin at the Savoy Experimental Watershed that feeds Langle and Copperhead Springs. Langle and Copperhead form an underflow-overflow system, where Langle receives all of the water from a nearby sinking stream at low flow, and Copperhead acts as an overflow route during high flow.

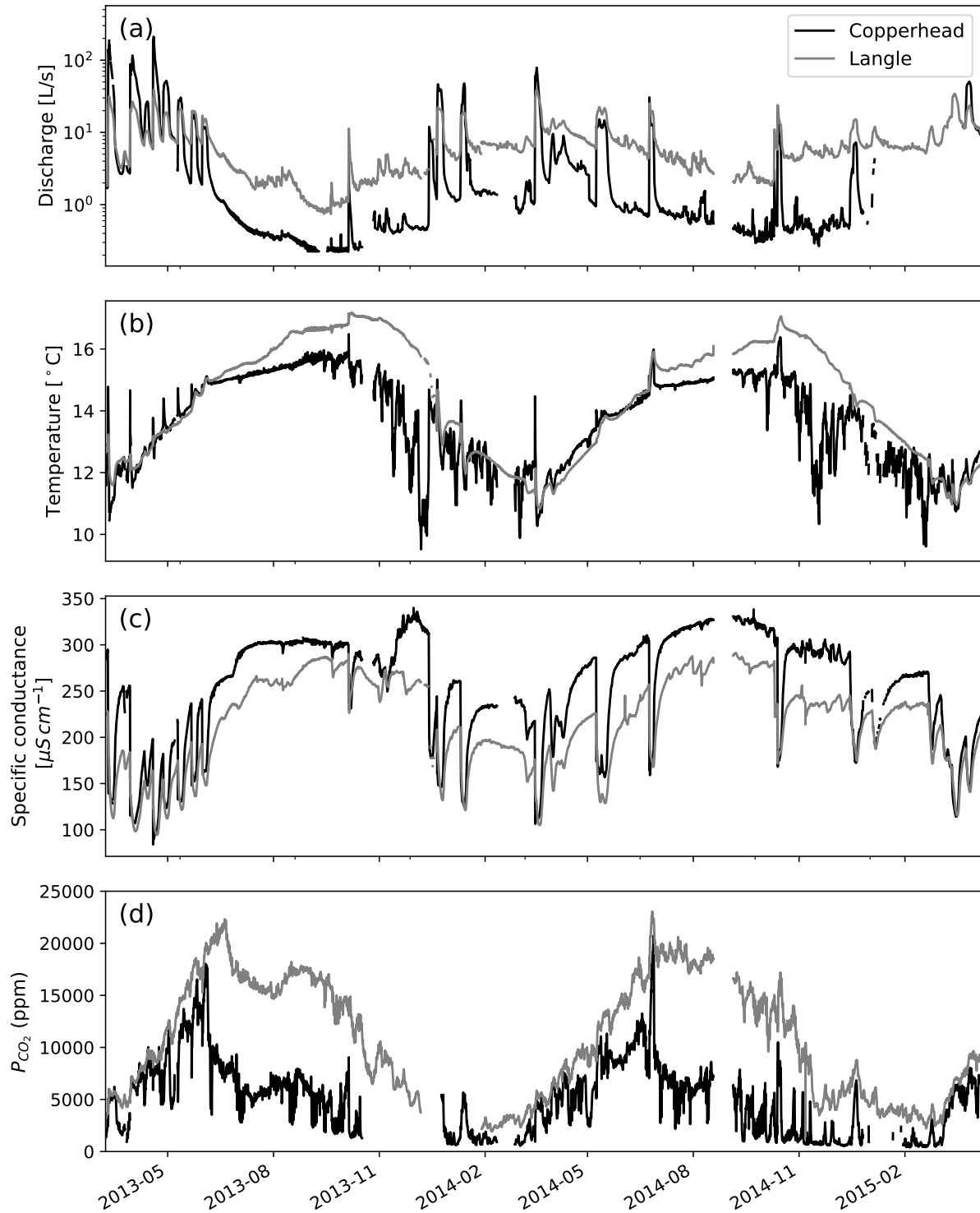


Figure 7: Time series data for the entire 2-year study period averaged over 90-min intervals for Copperhead and Langle Springs: (a) discharge, (b) water temperature, (c) specific conductance, and (d) partial pressure of dissolved  $CO_2$ . From Covington and Vaughn [2018]

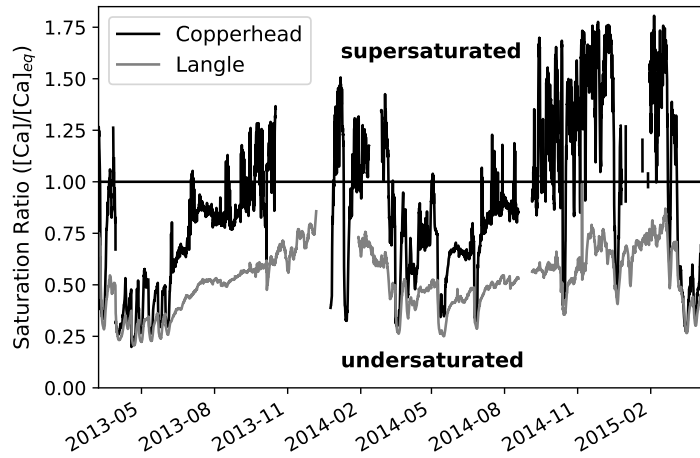


Figure 8: Saturation ratio with respect to calcite calculated from chemical time series at both springs. Langle Spring is undersaturated during the entire study period, whereas Copperhead Spring only spends about half of the time in undersaturated conditions. Copperhead Spring exhibits strong diurnal variability in saturation state during late summer to early winter. From *Covington and Vaughn [2018]*.

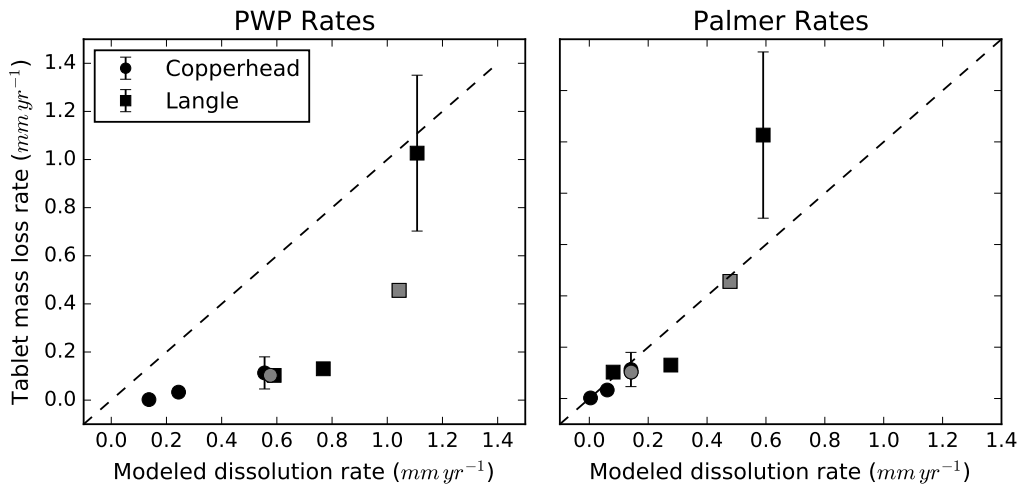


Figure 9: Comparison of measured mass loss rates of limestone tablets deployed at Copperhead (circles) and Langle (squares) Springs against the model rates calculated from the chemical time series data using the PWP and Palmer Equations. Each point represents the average rate of four tablets deployed at each spring, and the error bars indicate the standard error of the mean calculated from the variability among the tablets. Most tablets were deployed for three months, but the gray symbols indicate tablets deployed for six months. From *Covington and Vaughn [2018]*.

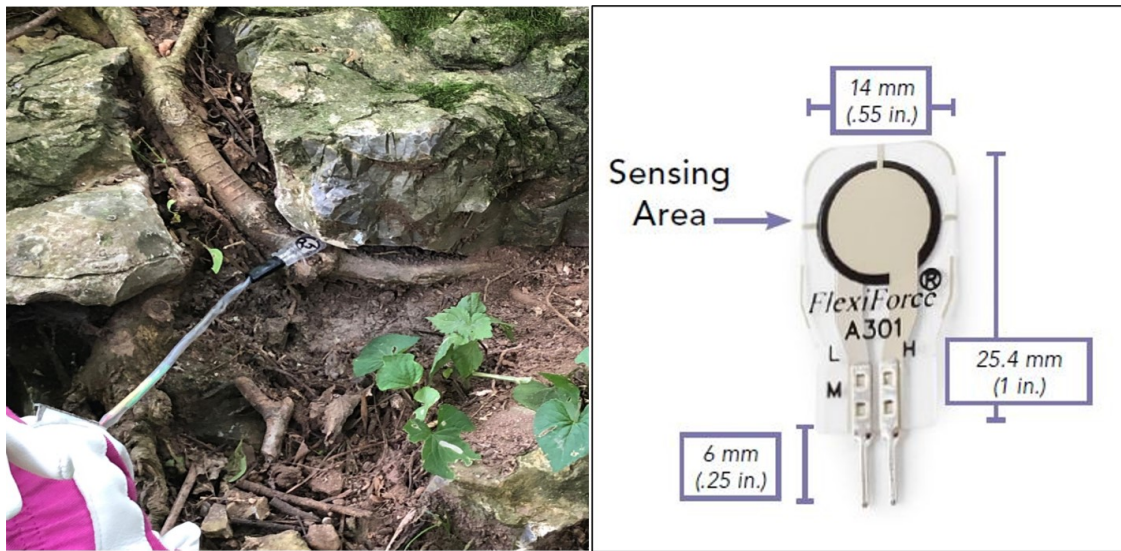


Figure 10: Force sensors used to instrument tree roots and measure the forces they exert on rock.

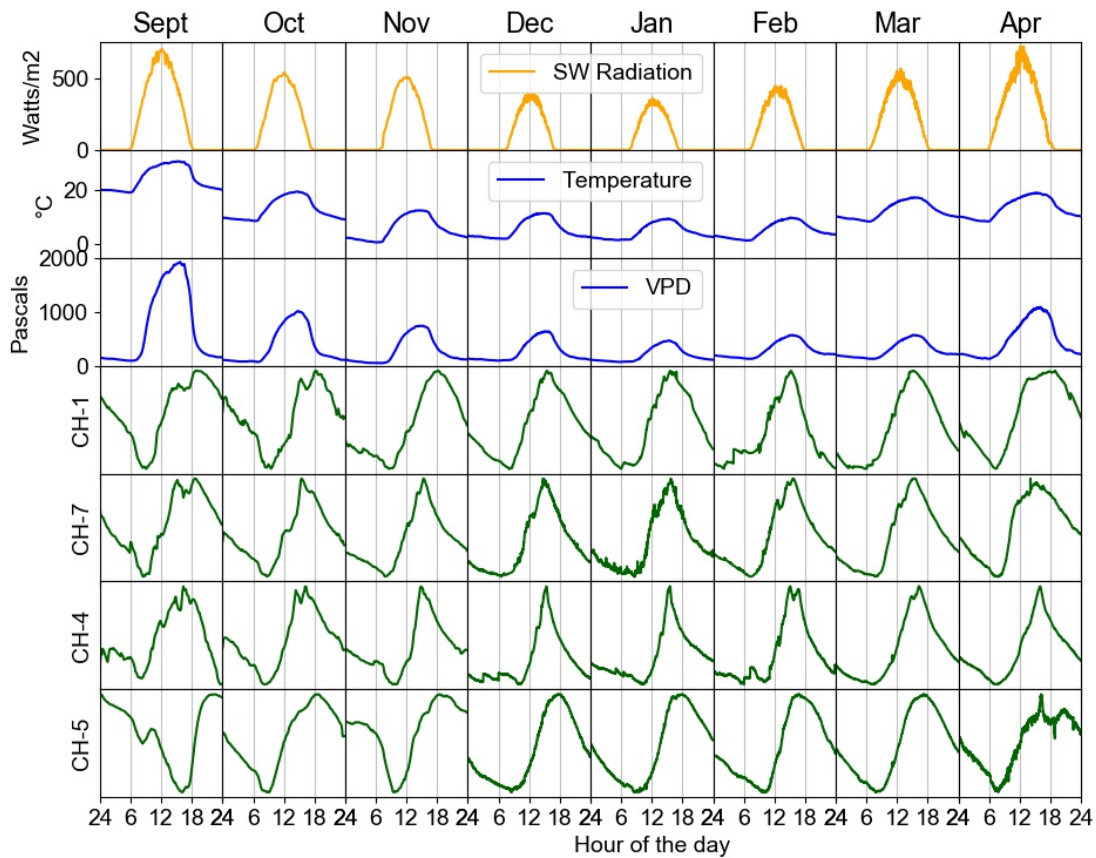


Figure 11: Seasonal patterns in force and potential drivers.

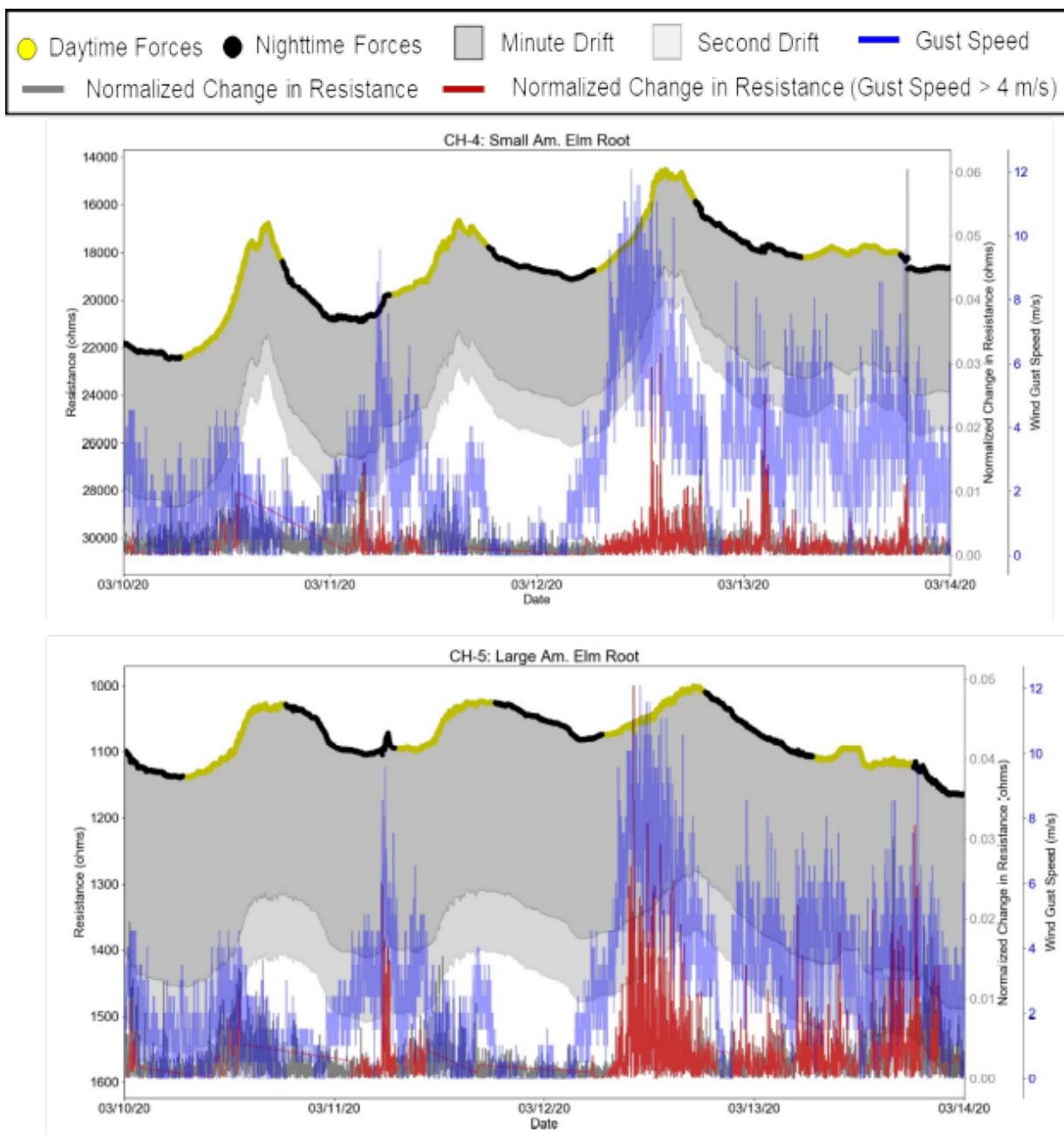


Figure 12: American elm roots (CH-4 and CH-5) forces and normalized change in forces (grey/red) during low, high, and sustained wind gust speeds. Force derivates in root forces are in grey when wind gusts are less than 4 m/s and when wind gusts exceeded 4 m/s are indicated in red. The yellow line indicates forces when solar radiation is active and black when it is absent. Grey region indicates the uncertainties in the possible resistance values that would be without drift.

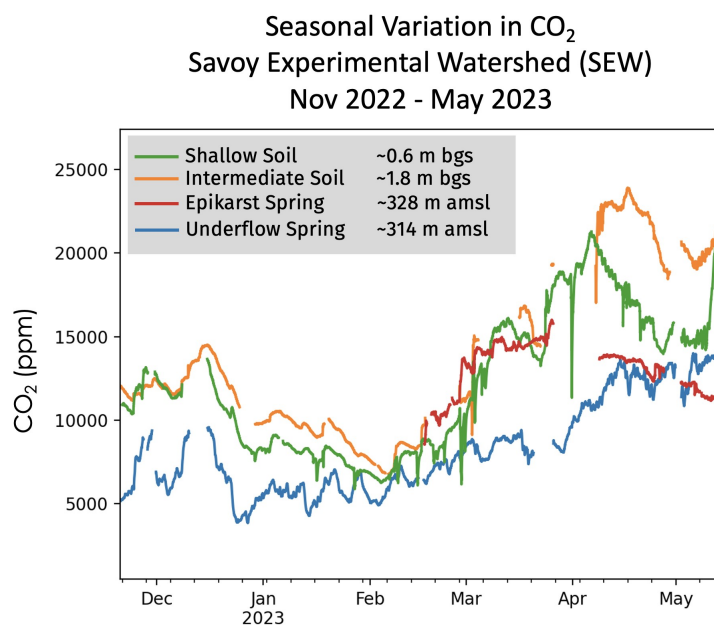


Figure 13: Seasonal patterns of  $CO_2$  at SEW show a decline in  $CO_2$  production during the non-growing season and an increase in  $CO_2$  during the growing season. Sharp dips and elevations in  $CO_2$  are due to changes in weather and are dependent on current hydrological conditions (i.e. soil moisture, spring discharge). Figure by M. Jones.

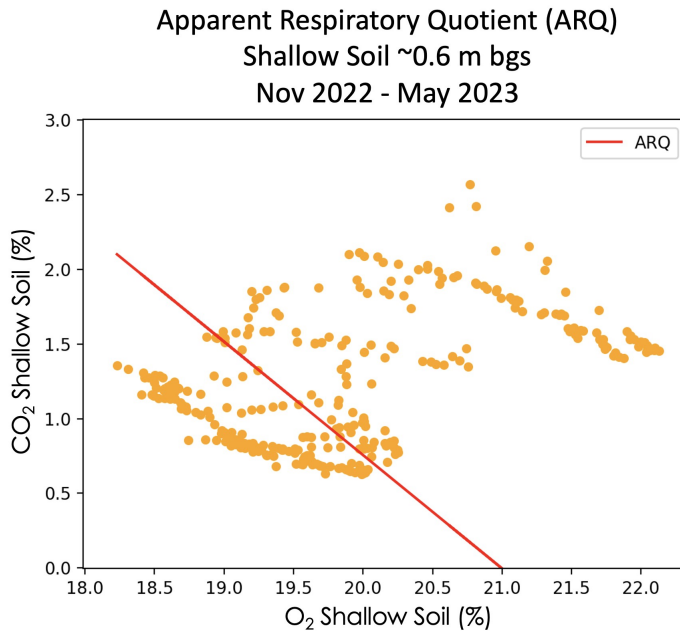


Figure 14: Plotted  $p\text{O}_2$  vs.  $p\text{CO}_2$  at the shallow soil (0.6 m bgs) in the SEW for November 2022 through May 2023. The red line corresponds to the theoretical relationship between  $p\text{O}_2$  and  $p\text{CO}_2$  ( $\text{ARQ}=1$ ) governed by diffusion and aerobic respiration, with a slope of -0.76 and x-intercept of 21. During the non-growing season, the shallower slopes fell below the theoretical relationship, which indicates a system depleted in  $\text{CO}_2$  through carbonate dissolution. During the growing season, the steeper slopes that fell above the theoretical relationship indicate a system enriched in  $\text{CO}_2$  through anaerobic respiration [Hodges *et al.*, 2019]. Figure by M. Jones.

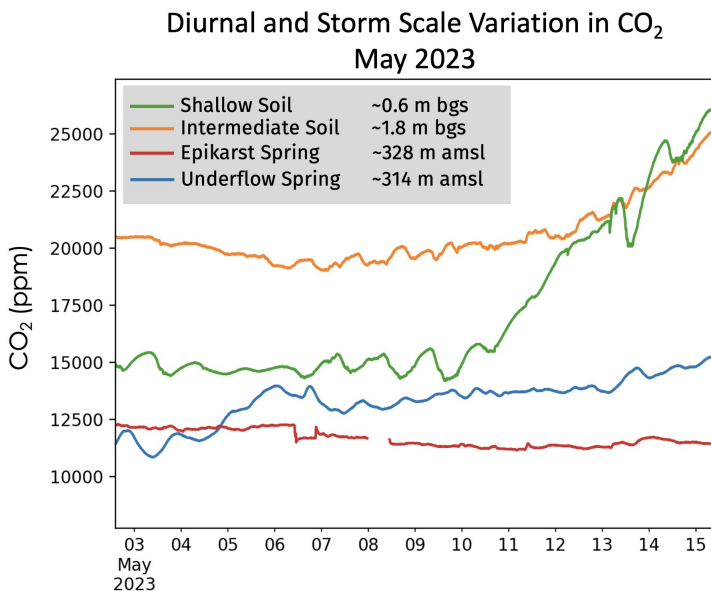


Figure 15: Variation in  $\text{CO}_2$  at SEW in May 2023 shows diurnal cycles and elevated  $\text{CO}_2$  following soil saturating spring thunderstorm events. Figure by M. Jones.

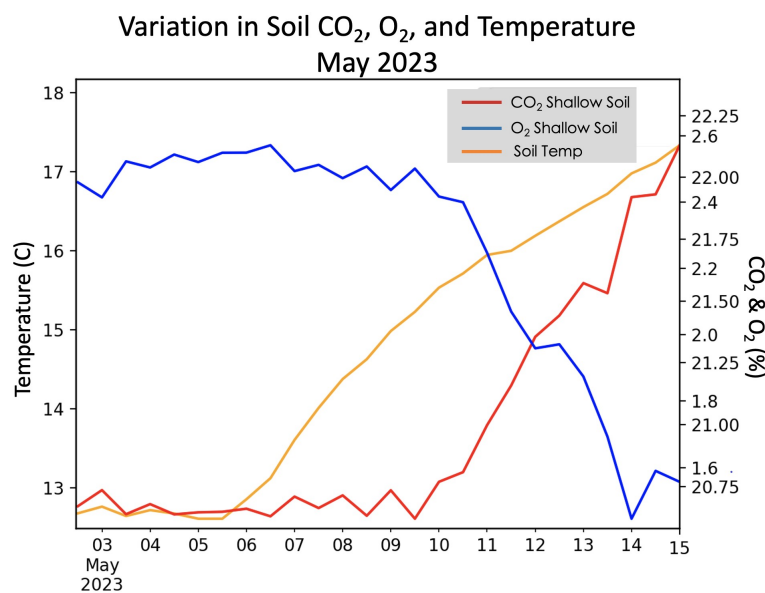


Figure 16: During May 2023, increasing soil temperatures and soil saturating spring showers cause an increase in  $CO_2$  production and depletion of  $O_2$  in the shallow soil (0.6 m bgs) at SEW. Figure by M. Jones.

## Blowing Springs Cave

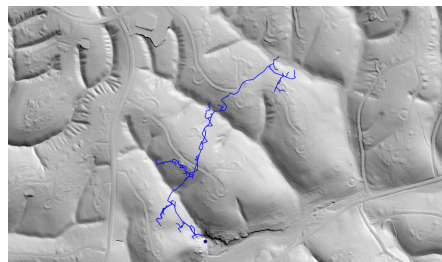


Figure 17: Hillshade with overlay of Blowing Springs Cave survey.

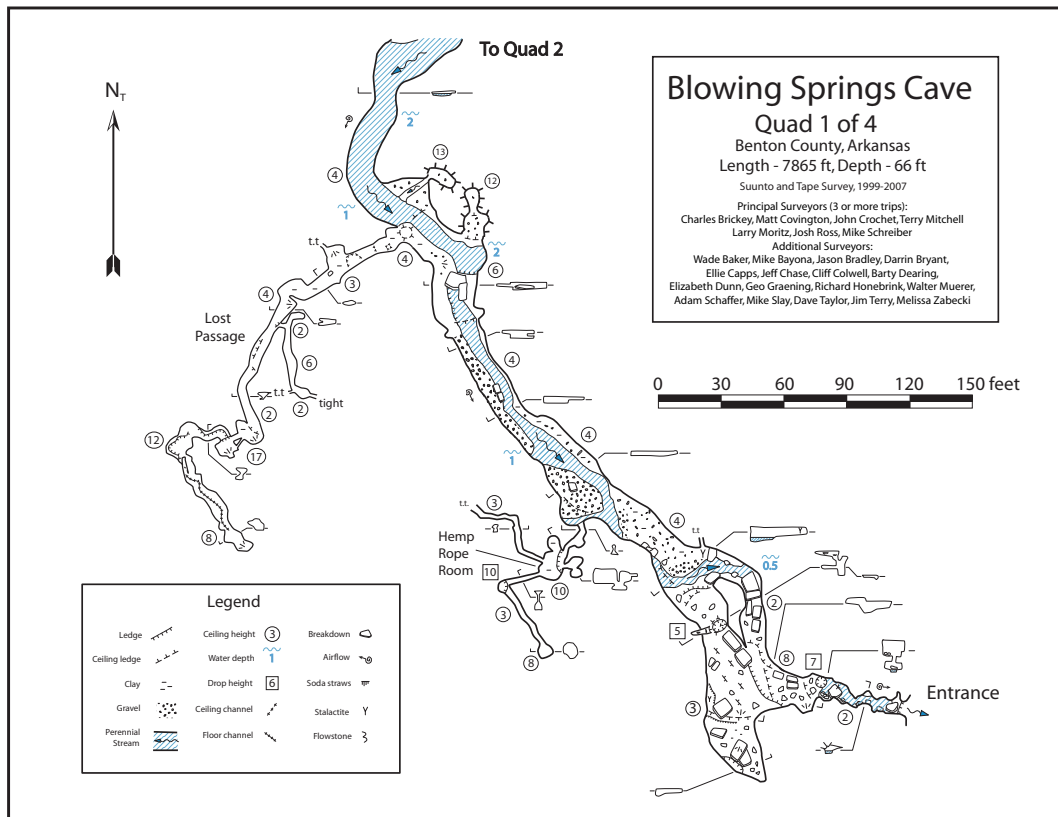


Figure 18: First quad of Blowing Springs Cave map.

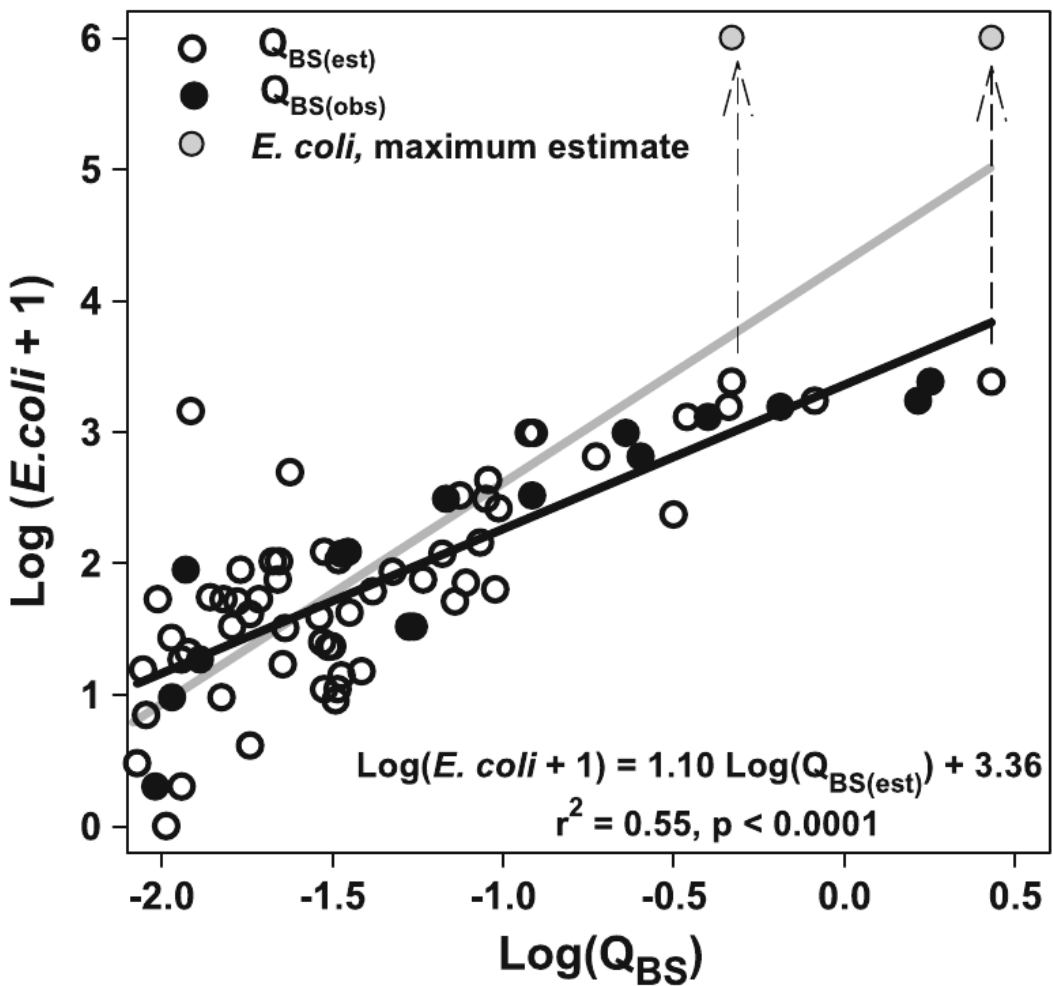


Figure 19: Log–log transformation of discharge versus *E. coli* concentration. The black line represents the regression between  $\text{log}(Q_{\text{BS}(\text{est})})$  and  $\text{log}(E.\text{coli} + 1)$ . The gray line represents a possible regression if the concentration for the two greatest, observed *E. coli* concentrations (i.e., 2420 MPN/100 mL) were 1,000,000 CFU/100 mL or MPN/100 mL, which is a maximum estimate of *E. coli* concentration in waste. From Knierim *et al.* [2015].

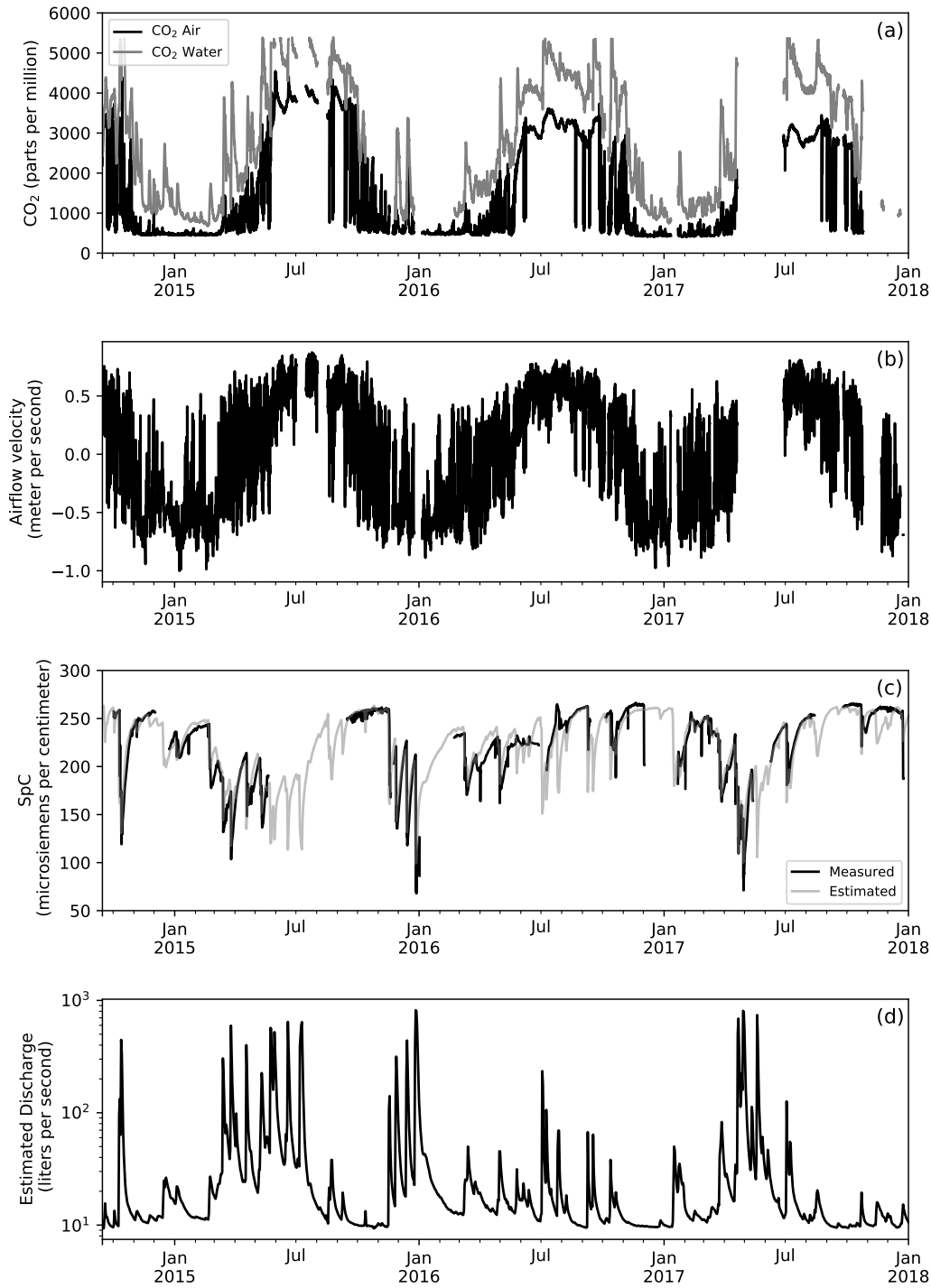


Figure 20: Time series data for the entire study period: (a) CO<sub>2</sub> concentrations in the air and water, (b) cave airflow velocity (positive values indicate the cave is blowing out), (c) specific conductance in the cave stream (black) and an estimated daily specific conductance using a regression to discharge (gray), and (d) estimated discharge of the cave calculated from streamflow at Little Sugar Creek. From *Covington et al. [2020]*.

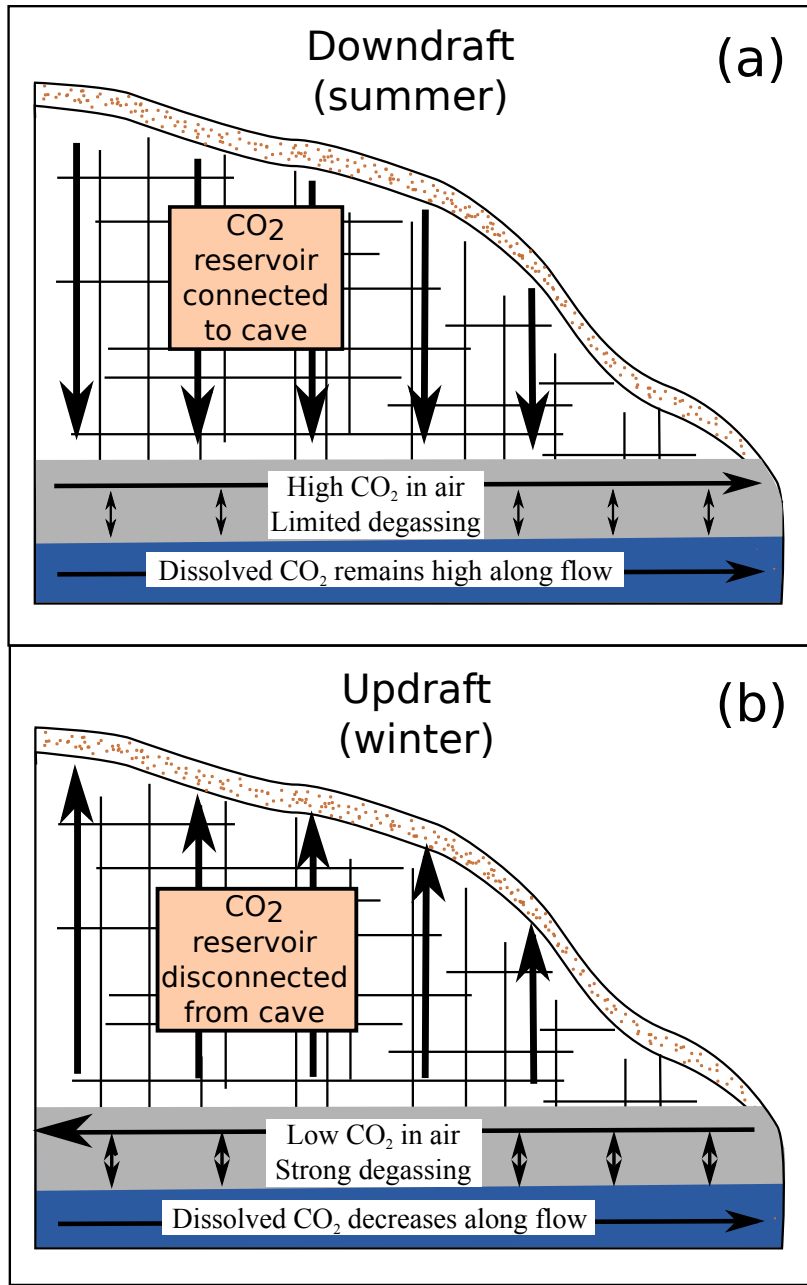


Figure 21: Conceptual model of how ventilation direction impacts dissolution rates in the cave stream: (a) During downdraft (summer conditions), air flows vertically downward through the soil and unsaturated zone, obtaining high CO<sub>2</sub>. Cave air pCO<sub>2</sub> is high and therefore degassing of CO<sub>2</sub> from the cave stream is limited. Consequently, dissolved CO<sub>2</sub> and dissolution rates remain high along the main conduit. (b) During updraft (winter conditions), atmospheric air enters the cave through the large lower entrance and then flows upward through the high-CO<sub>2</sub> unsaturated zone. The cave air is disconnected from this high CO<sub>2</sub> zone and strong degassing of CO<sub>2</sub> occurs along the stream, reducing pCO<sub>2</sub> and dissolution rates. During winter storms, vertical flow of water can transport CO<sub>2</sub> through the unsaturated zone and effectively reconnect the cave stream to the CO<sub>2</sub> reservoir. From Covington *et al.* [2020].

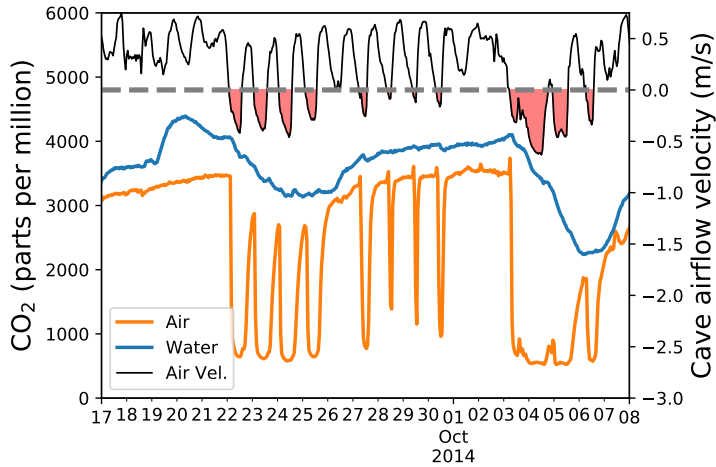


Figure 22: Time series of airflow velocity (top, black), and CO<sub>2</sub> concentrations in air (orange, bottom) and water (blue, middle), where the gray dashed line demarcates zero airflow velocity and the shaded red portions of the curve are periods of updraft (inward airflow). During updraft, gaseous CO<sub>2</sub> concentrations decrease sharply to near atmospheric concentrations. During extended periods of updraft, dissolved CO<sub>2</sub> also decreases. During downdraft CO<sub>2</sub> in the air and water increase. From Covington *et al.* [2020].

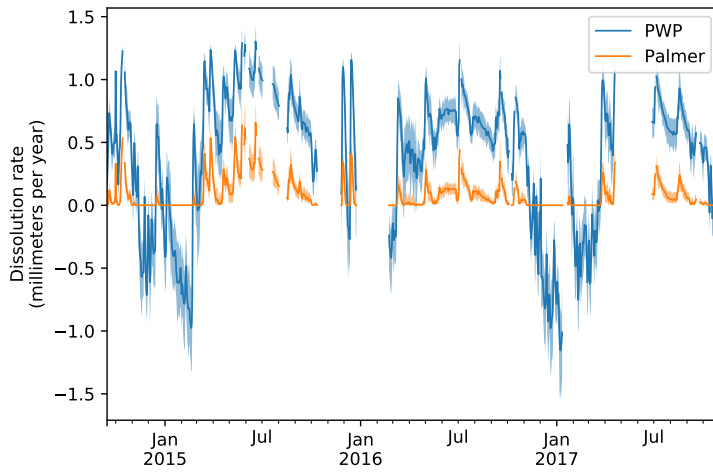


Figure 23: Calcite dissolution rates calculated from pCO<sub>2</sub> and SpC time series, where the blue line depicts rates calculated using the PWP equation (which includes negative values) and the yellow line indicates rates calculated using the Palmer equation. The shaded bands indicate a 90% confidence interval based on the Monte Carlo error propagation. The data indicate a regular seasonal pattern in dissolution rate variability, with undersaturated conditions typical in the summer and supersaturated conditions typical in the winter. From Covington *et al.* [2020].

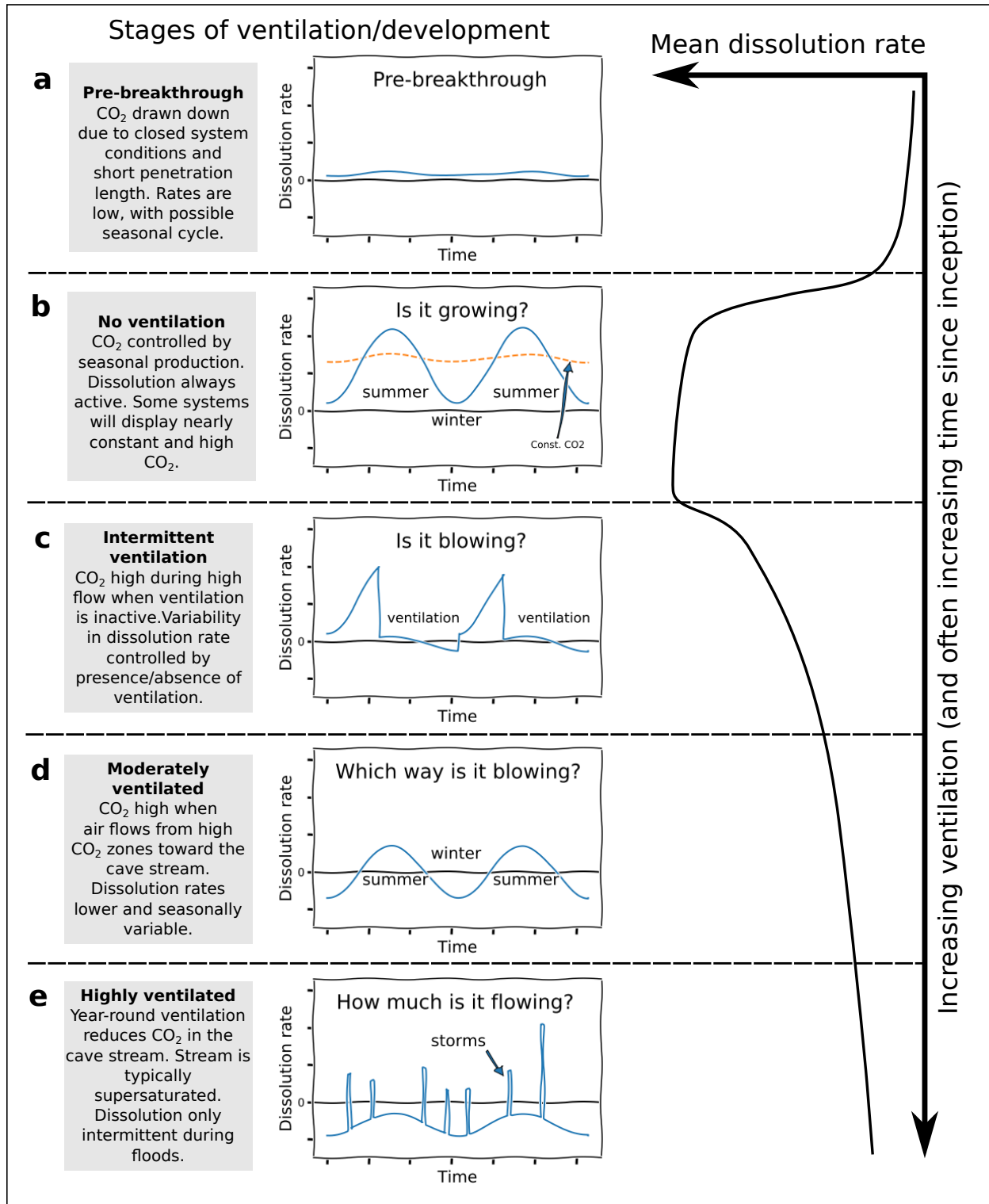


Figure 24: Patterns of observed dissolution rate variation from this and other studies and how they relate to ventilation strength and resulting CO<sub>2</sub> dynamics. Except during periods of base-level aggradation, caves will typically evolve toward being more ventilated over time. From Covington *et al.* [2020].

## Cave Springs Cave

Cave Spring Cave (Figure 25) provides habitat for the largest population of Ozark Cavefish known. The Ozark Cavefish (Figure 26) is a small fish, reaching a maximum total length of 50 mm (2 inches). The species is adapted to subterranean habitats and features characteristics of life underground such as loss of pigment, eyes, and enhanced sensory structures such as the lateral line system which helps it navigate and find prey in total darkness. This cavefish is restricted to the Springfield Plateau and historically occurred at approximately 53 sites. In Arkansas, Ozark Cavefish are found in Benton County and 1 site in Washington County.

At Cave Springs Cave, studies on the Ozark Cavefish have been ongoing since the 1950's when Tom Poulson visited the cave during his dissertation research. The earliest population estimate was a pre-1955 estimate of 150 cavefish prior to the collections made by Tulane University. From 1955-1957, researchers from Tulane collected 128 specimens. During this time period and into the early 1960's, the number of cavefish observed (and/or collected) was low with the exception of 1960 when 93 cavefish were observed. Scientific collection was one of threat included when this species as listed as a federally threatened species in 1984. Over-collection of cavefish appears to have depressed the Cave Springs Cave population for a time period; however, surveys from the 1980s to 2012 suggest a return to pre-1955 population size (Figure 27).

In addition to Ozark Cavefish, the cave provides habitat for about 50 species including a small maternity colony of Gray Bats (federally endangered species), salamanders such as the Western Grotto Salamander and Cave Salamander, and rare, obligate cave invertebrate species such as cave amphipods and cave isopods.

Conservation efforts at Cave Springs Cave have focused on 3 main areas: 1.) controlling access to the cave; 2.) acquiring high priority land parcels that protect the entrance, cave passages, and bat flyways (Figure 28); and 3.) managing appropriate land use in the recharge area (Figure 29). A bat friendly fence was installed around the entrance to reduce illegal human visitation but allow bats to move freely. The entrance and parcels above the known cave passages were acquired by Arkansas Natural Heritage Commission and are managed as a state Natural Area, and Illinois River Watershed Partnership acquired the spring run and lake which protects the bat flyway. Delineating the recharge area for Cave Springs Cave has been an important tool for historic and ongoing conservation planning. Examples of how recharge delineation has benefitted Cave Springs Cave include early studies that shifted the I-49 interstate out of the direct recharge portion of the recharge area and a more recent study that resulted in municipalities incorporating additional best management practices into existing storm water and drainage regulations for any new construction within the recharge area.



Figure 25: Entrance of Cave Springs Cave after heavy precipitation event.



Figure 26: Ozark Cavefish. Photo by Missouri Department of Conservation

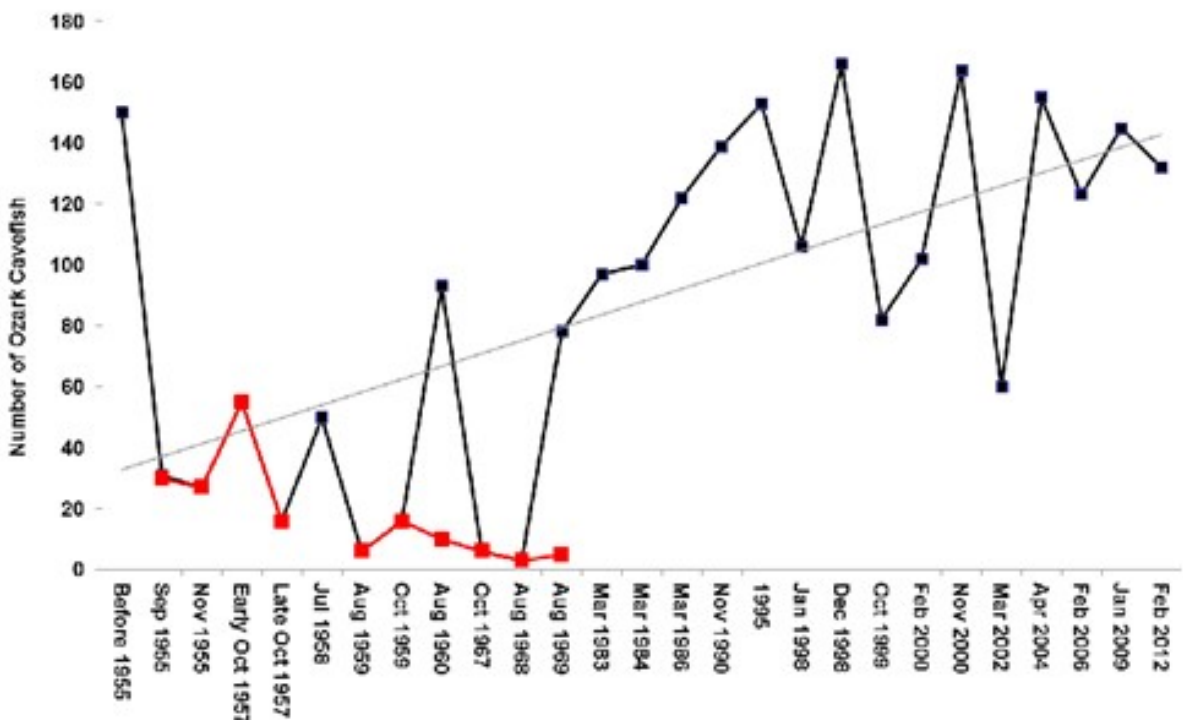


Figure 27: Ozark Cavefish counts, 1955-2012 in Cave Springs Cave. Note: The black line represents the total count while the red line represents the number taken, a practice that was discontinued in 1969. Trend line show demonstrates increase in population over time.

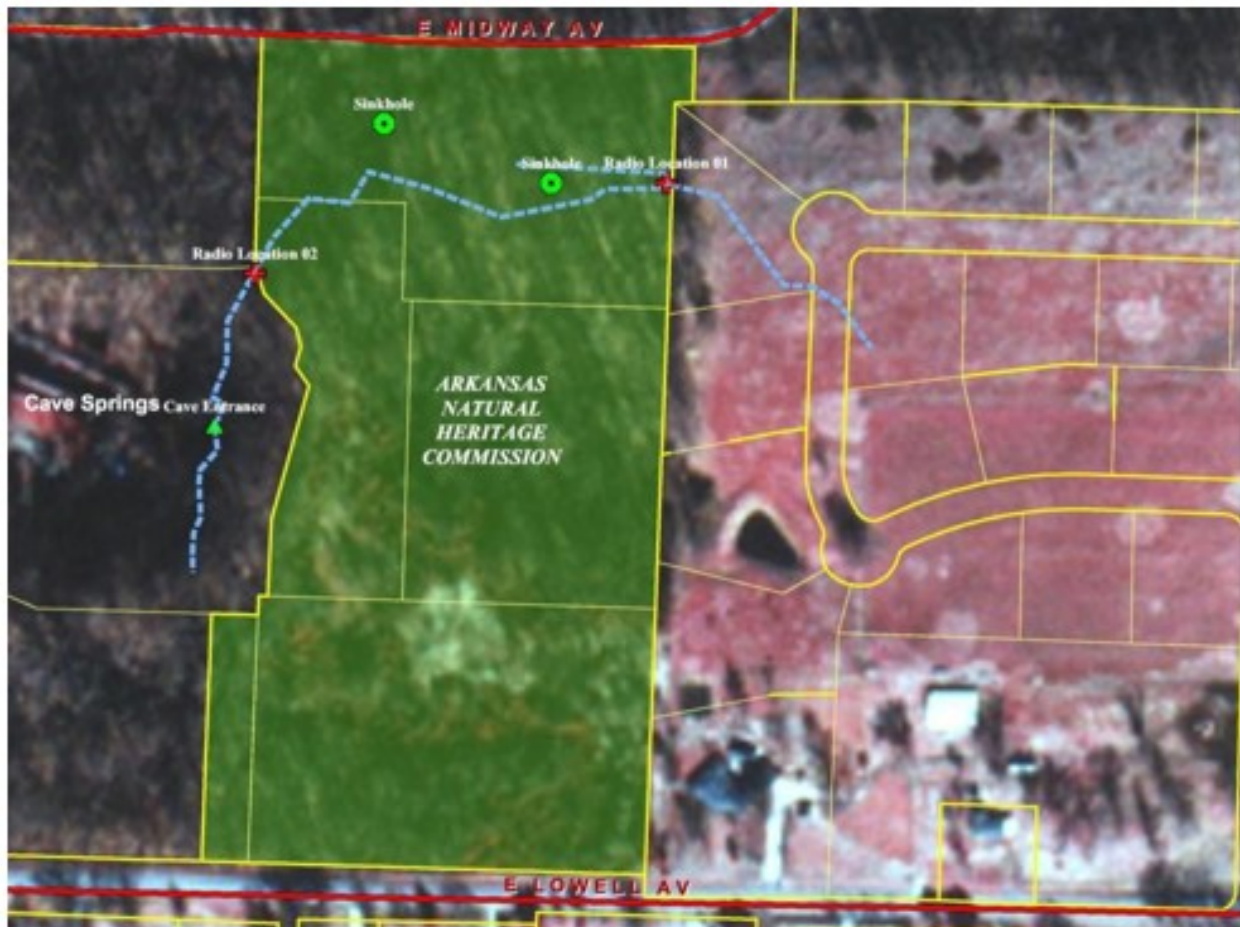


Figure 28: A cave radio was used to confirm which land parcels were above known cave passages.

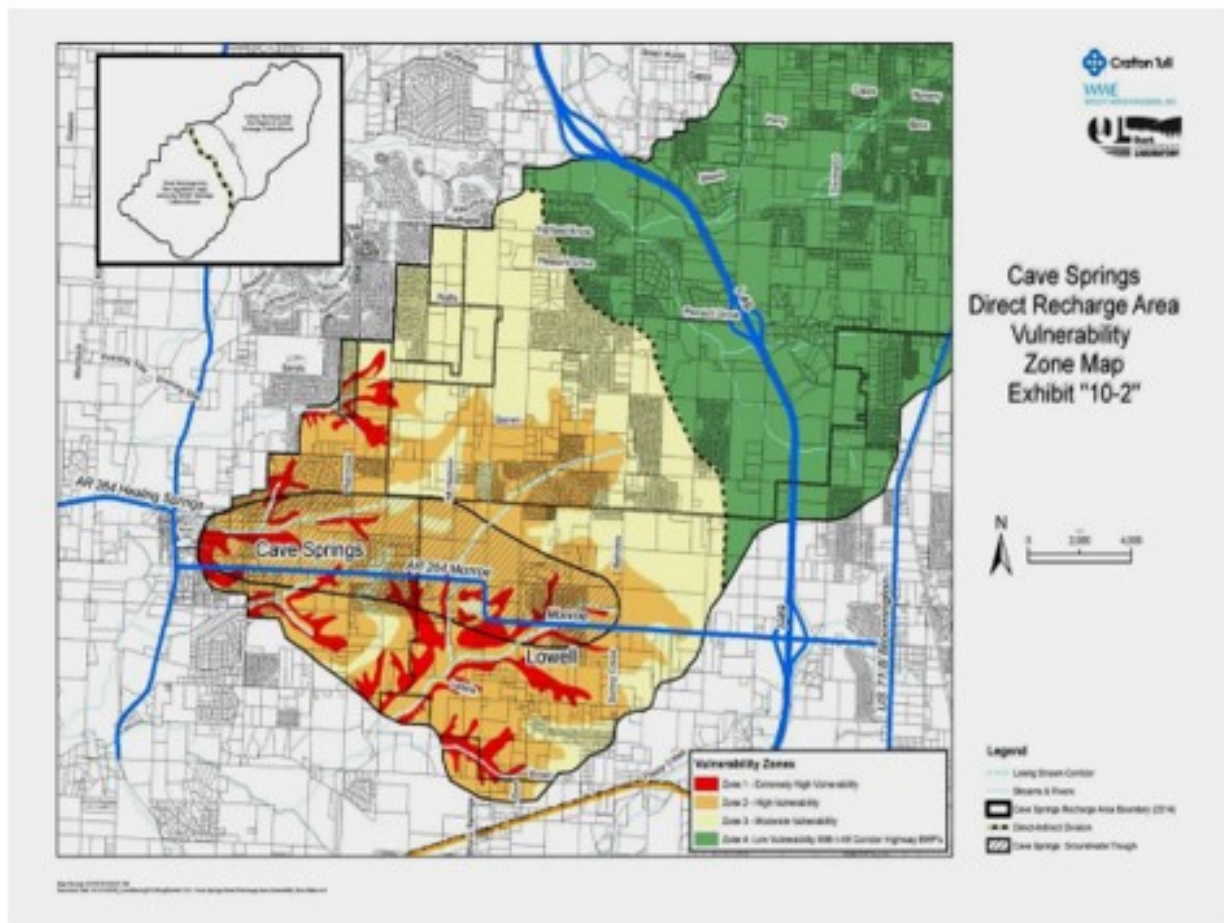


Figure 29: Recharge delineation for Cave Springs Cave showing vulnerability categories.

## References

- Brahana, J., P. Hays, T. Kresse, T. Sauer, and G. Stanton, The savoy experimental watershed—early lessons for hydrogeologic modeling from a well-characterized karst research site, *Karst modeling, Karst Waters Institute Special Publication*, 5, 247–254, 1999.
- Brahana, V., *Ten relevant karst hydrogeologic insights gained from 15 years of in situ field studies at the Savoy Experimental Watershed*, pp. 132–141, U.S. Geological Survey Scientific Investigations Report 2011-5031, 2011.
- Covington, M. D., and K. A. Vaughn, Carbon dioxide and dissolution rate dynamics within a karst underflow-overflow system, Savoy Experimental Watershed, Arkansas, USA, *Chemical Geology*, p. 118689, 2018.
- Covington, M. D., K. Knierim, H. A. Young, J. Rodriguez, and H. Gnoza, Cave airflow patterns control calcite dissolution rates within a cave stream: Blowing Springs Cave, Arkansas, USA, *Preprint*, EarthArXiv, 2020.
- Covington, M. D., J. B. Martin, L. E. Toran, J. L. Macalady, N. Sekhon, P. L. Sullivan, A. García Jr., J. B. Heffernan, and W. D. Graham, Carbonates in the critical zone, *Earth's Future*, 11, e2022EF002,765, 2023, e2022EF002765 2022EF002765.
- Hodges, K., S. Brantley, and J. Kaye, Soil  $CO_2$  and  $O_2$  concentrations illuminate the relative importance of weathering and respiration to seasonal soil gas fluctuations, *Soil Science Society of America Journal*, 83, 1167 – 1180, 2019.
- Hudson, M. R., Coordinated strike-slip and normal faulting in the southern ozark dome of northern arkansas: Deformation in a late paleozoic foreland, *Geology*, 28, 511–514, 2000.
- Hudson, M. R., and K. J. Turner, Late paleozoic flexural extension and overprinting shortening in the southern ozark dome, arkansas, usa: Evolving fault kinematics in the foreland of the ouachita orogen, *Tectonics*, 41, e2021TC006,706, 2022.
- Knierim, K. J., P. D. Hays, and D. Bowman, Quantifying the variability in escherichia coli (e. coli) throughout storm events at a karst spring in northwestern arkansas, united states, *Environmental earth sciences*, 74, 4607–4623, 2015.
- Stanton, G., Processes and controls affecting anisotropic flow in the boone-st. joe aquifer in northwest arkansas, Master's thesis, University of Arkansas, 1993.